Available online at www.sciencedirect.com
ScienceDirect
Catalysis Today 121 (2007) 217–225
CATALYSIS TODAY
www.elsevier.com/locate/cattod

Transient analysis of the release and reduction of NO_x using a $Pt/Ba/Al_2O_3$ catalyst

Yoshiyuki Sakamoto *, Tomoyoshi Motohiro, Shinichi Matsunaga, Kohei Okumura, Tomoyuki Kayama, Kiyoshi Yamazaki, Toshiyuki Tanaka, Yoshimi Kizaki, Naoki Takahashi, Hirofumi Shinjoh

TOYOTA Central Research & Development Labs., Inc., Nagakute, Aichi 480-1192, Japan

Available online 7 July 2006

Abstract

The release and reduction of NO_x in a NO_x storage-reduction (NSR) catalyst were studied with a transient reaction analysis in the millisecond range, which was made possible by the combination of pulsed injection of gases and time resolved time-of-flight mass spectrometry. After an O_2 pulse and a subsequent NO pulse were injected into a pellet of the $Pt/Ba/Al_2O_3$ catalyst, the time profiles of several gas products, NO, N_2, NH_3 and H_2O, were obtained as a result of the release and reduction of NO_x caused by H_2 injection. Comparing the time profiles in another analysis, which were obtained using a model catalyst consisting of a flat 5 nm$Pt/Ba(NO_3)_2$/cordierite plate, the release and reduction of NO_x on $Pt/Ba/Al_2O_3$ catalyst that stored NO_x took the following two steps; in the first step NO molecules were released from Ba and in the second step the released NO was reduced into N_2 by H_2 pulse injection. When this H_2 pulse was injected in a large amount, NO was reduced to NH_3 instead of N_2.

A only small amount of H_2O was detected because of the strong affinity for alumina support. We can analyze the NO_x regeneration process to separate two steps of the NO_x release and reduction by a detailed analysis of the time profiles using a two-step reaction model. From the result of the analysis, it is found that the rate constant for NO_x release increased as temperature increase.

Keywords: Time-of-flight mass spectrometry; NSR catalyst; Cordierite plate

1. Introduction

Lean-burn and diesel engines have great potentials in overcoming the problems of environmental pollution and fuel economy. However, conventional three-way catalysts are ineffective in removing NO_x from the exhaust gas of these engines, which contains a large amount of oxygen. One effective method that solves this problem is the use of a NO_x storage-reduction (NSR) catalyst [1–5].

NSR catalysts remove NO_x by alternating the composition of the exhaust gas between lean and rich. During the lean period of operation, the catalyst stores NO_x as species of nitrites and nitrates. A short pulse of rich gas is injected so that the stored NO_x is released and reduced to N_2. It is generally accepted that this NSR process can be separated into five elemental reactions [6,7]:

(1) NO oxidation to NO_2 [8,9].
(2) NO_x storage on the catalyst surface [10,11].
(3) Evolution of reductant.
(4) NO_x release from the storage site.
(5) NO_x reduction to N_2.

Despite the general acceptance of this process, the detailed mechanisms are not fully understood, especially the release and reduction of NO_x. From a practical point of view, it has been reported that at relatively low temperature the NO_x storage capacity is sufficient, but that the rate of NO_x release and reduction, sometimes called the NO_x regeneration, is slow and insufficient [12]. Analysis of the NO_x regeneration is more difficult than that of NO oxidation and NO_x storage, because the regeneration accompanied by pulse injection of rich gas is completed in an extremely short period. Another reason for this difficulty is that the main reaction product is N_2, which is a significant constituent in real exhaust gases and is usually used for the diluent gas in the laboratory.

Although some studies of transient reaction have been done using He as a diluent gas [10,13–15], it seems that with this

* Corresponding author. Tel.: +81 561 63 5283; fax: +81 561 63 5260.
E-mail address: sakamoto@mosk.tytlabs.co.jp (Y. Sakamoto).

0920-5861/$ – see front matter
doi:10.1016/j.cattod.2006.05.088

method the time resolution of the measurement was too low even to obtain the time profile of the main product, N_2. The aim of the present study is to develop a method to obtain the time profile of N_2 with millisecond resolution. Moreover, we would like to improve our understanding of the NO_x regeneration process.

Motohiro et al. developed a dynamic vacuum system for transient reaction analysis of a flat type catalyst on a millisecond timescale (which is essentially a time-resolved time-of-flight mass spectrometry with molecular-pulse-probe for reaction analysis at the surface of catalysts named TM+ since the output raw data is essentially the amount of reaction product cations (+) mapped on the time (T) and mass (M) space) [16–18]. The TM+ system has also blanched out to analyze the transient reaction of a pellet type catalyst [19,20] by reference to the TAP (temporal analysis of products) reactor [21]. We applied both reactor systems in our NSR analysis.

2. Experimental

2.1. Preparation of a Pt/Ba(NO$_3$)$_2$/cordierite plate for analyzing the decomposition of Ba(NO$_3$)$_2$

Pt and Ba were chosen, respectively, as the precious metal and the NO_x storage component for our study because they are well-accepted materials for NSR catalysts.

We prepared two kinds of samples for our study, a flat sample and a pellet sample. The latter is described in the next section. The flat sample, 5 nmPt/Ba$(NO_3)_2$/cordierite, was fabricated starting with a square cordierite plate, 50 mm on a side and 5 mm thickness. A saturated solution of Ba $(NO_3)_2$ (Wako Pure Chemical Industries) of 5 cm^3 was dropped onto the plate, which was then dried in vacuum at room temperature overnight. The resultant sample was then placed in an ultra high vacuum chamber and was sputter-coated with platinum at the amount equivalent to 5 nm in thickness. The resultant sample named 5 nmPt/Ba$(NO_3)_2$/cordierite plate was deemed to be a model NSR catalyst, saturated with sites for NO_x storage.

2.2. Preparation of a pellet type Pt/Ba/Al$_2$O$_3$ catalysts for NSR analyses

Pellets of Pt/Ba/Al_2O_3 catalyst were prepared using a two-step wet impregnation method. Firstly, powdery γ-Al_2O_3 (Nikki Universal, 150 m^2/g) was wet impregnated with $Pt(NH_3)_2(NO_2)_2$ (Tanaka Precious Metals). This material was filtered, washed, dried at 393 K for 12 h, and calcined at 573 K for 3 h in the air. We call this a Pt/Al_2O_3 sample. Secondly, a portion of this sample was stirred into an aqueous solution containing $Ba(CH_3COO)_2$ (Wako Pure Chemical Industries) and the excess water was removed by heating while continually stirring, The resultant powder was dried at 393 K for 12 h and calcined at 773 K for 3 h in the air. The amount of Pt and Ba per 120 g γ-Al_2O_3 was 2 g and 0.2 mol, respectively. The powder sample was pressed and sieved to make pellets of 0.7–1.0 mm diameter.

2.3. Transient reaction analysis of a flat type catalyst

A flat plate sample of 5 nmPt/Ba$(NO_3)_2$/cordierite was placed in the TM+ apparatus shown in Fig. 1. The apparatus was equipped with four pulsed valves, two cryopumps for vacuum chambers placed sample, and two turbo pumps for differentially pumped down chambers and time-of-flight mass spectrometer (TOF-MS). The sample was fixed in a holder with a flat heater and the surface temperature was maintained at 350 °C. Pulses of pure H_2 gas with a volume of 0.2 cm^3 and pulse width of 1 ms were supplied to release and reduce the Ba$(NO_3)_2$ in the sample. The reason for choosing H_2 was because this is the most effective gas for regeneration of stored NO_x at low temperature [22] and because its simple mass peaks of H_2 and prospective products makes the analysis of the mass spectra easy. The chambers were kept under high vacuum: the first chamber, where the samples were placed, was at about 10^{-6} Pa; the differential chamber at 10^{-7} Pa, and the chamber for TOF-MS at 10^{-8} Pa. The intensity of each mass peak was calibrated using mass spectral data [23].

The measurement procedure was as follows. After injecting pulse of H_2, a part of the reaction products emitted from the catalyst was sampled through a skimmer located in the direction normal to the plane surface of the catalyst. The reaction products were ionized and detected by the TOF-MS on a millisecond scale. This procedure of H_2 gas pulsing and detection of the gas products was repeated 100 times with a period of 5 s in order to improve the signal to noise ratio by averaging the accumulated data. The amount of reaction products and NO_x in the sample decreased gradually as the progress of Ba$(NO_3)_2$ decomposition by H_2 gas pulsing because NO_x was not supplied to the sample during the measurement. The averaging data were the result of the averaging of the products for 100 times of the measurement, though the amount of the products of each measurement was decreased as the progress of Ba$(NO_3)_2$ decomposition. The elemental ratio of the sample surface was measured by X-ray photoelectron spectroscopy (XPS) before and after the H_2 pulsing experiment.

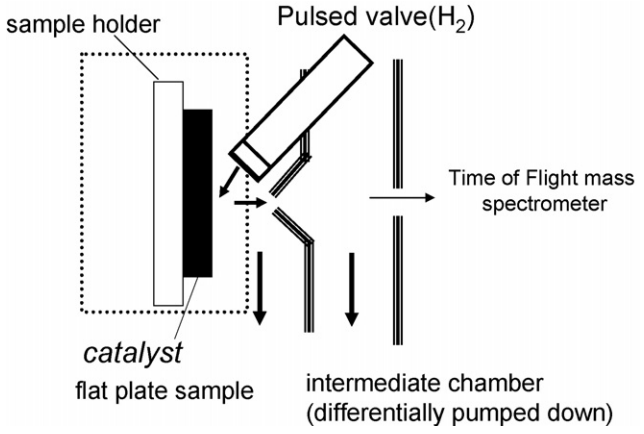

Fig. 1. TM+ apparatus for a flat plate sample. Pulses of reactant gases are supplied through valves. The catalyst sample is set in ultra high vacuum conditions. The gases are analyzed with time-of-flight mass spectrometry through a differentially pumped-down intermediate chamber.

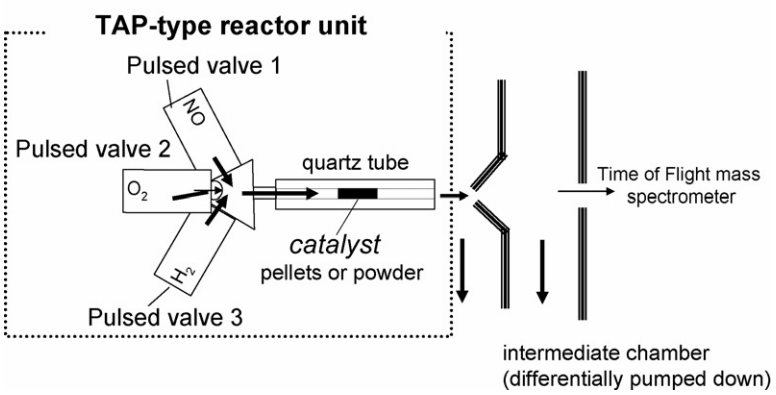

Fig. 2. TAP-type reactor apparatus for NSR analysis. Pulses of the reactant gases, NO, O_2 and H_2, are supplied through three separate valves. Catalyst in the form of pellets or powder is placed into a quartz tube. The gases are analyzed in the same way as shown in Fig. 1.

2.4. Transient reaction analysis of a pellet type catalyst

A 0.2 g pellet of $Pt/Ba/Al_2O_3$ catalyst was inserted into a quartz tube with a 4.5 mm internal diameter and a length of 38 mm, as shown in Fig. 2. Silica wool was stuffed into both ends of the quartz tube. A simplified schematic diagram of the TAP-type reactor apparatus is shown in Fig. 2 [19,20], which is installed in the TM+ system mentioned in Section 2.3. The quartz tube containing the catalyst was installed in this vacuum system, which was evacuated to 10^{-7} Pa. The tube was then heated with an external heater up to a preset temperature. For this analysis, we used three valves for the gas pulses, one each for pure O_2, NO and H_2 gases. The amount of gas in the pulse could be controlled either by the pulse width or by the backpressure of the valve. In this case, the amount of gas was controlled by the backpressure of the valve. The measured pulse width was broader than 1.0 ms preset by a pulsed valve controller because of a gas diffusion effect; nevertheless all the pulse widths were set to 1.0 ms by a pulsed valve controller. The amount of O_2 and NO was fixed at about 0.8 and 1.0 cm^3 per pulse, respectively. The amount of Ba for NO_x storage was calculated to be 3×10^{-7} mol per 0.2 g catalyst, whereas the amount of NO was 3×10^{-4} mol per pulse. Thus, the amount of NO was altogether sufficient for the amount of Ba. The amount of H_2 was varied from 0.1 to 0.4 cm^3 per pulse by changing the backpressure of the valve.

The measurement procedure used for this analysis was similar to that used for TM+ type analysis of the flat type catalyst in Section 2.3, and was as follows. After maintaining the catalyst at a preset temperature, an O_2 pulse was injected to the catalyst followed by a NO pulse injection with an interval of 100 ms. This procedure models the NO_x storage step, which involves oxidation of NO into NO_2 and storage of NO_x. H_2 was injected to the catalyst 5 s after the injections of O_2 and NO pulses in order to bring about NO_x regeneration. The NO_x storage step was repeated again 200 ms after the H_2 injection. The NO_x storage and regeneration was repeated 30 times in order to improve the signal to noise ratio as was done for the analysis of the flat type catalyst. The reactant and product gases were detected for 200 ms after the O_2 pulse injection and for 200 ms after the H_2 pulse injection. In order to accumulate data after the reaction stabilized, the same measurement procedure was repeated 30 times as a pretreatment.

3. Results

3.1. $Ba(NO_3)_2$ decomposition analysis

H_2O, NH_3, N_2 and NO were detected with H_2 injection to the flat sample of the 5 nmPt/$Ba(NO_3)_2$/cordierite in the TM+ type measurement as shown in Fig. 3, however N_2O and NO_2 were not detected. When the $Ba(NO_3)_2$/cordierite without Pt was also

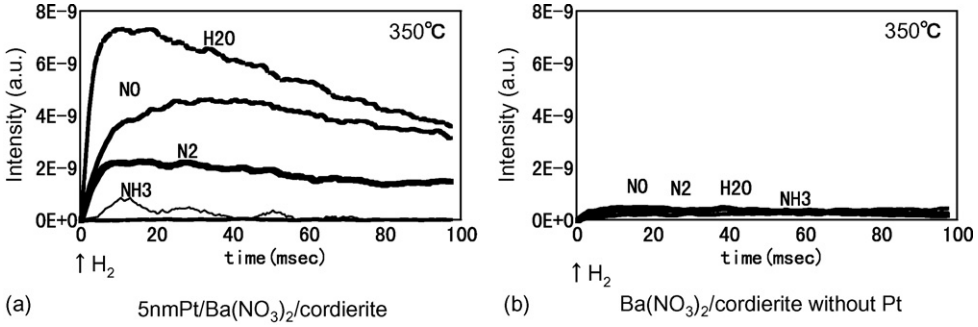

Fig. 3. Time profiles of the gas products generated as a result of $Ba(NO_3)_2$ decomposition from supplying pulses of H_2 gas to: (a) a flat type sample of 5 nmPt/$Ba(NO_3)_2$/cordierite ($2MgO{\cdot}2Al_2O_3{\cdot}5SiO_2$) and (b) a flat type sample of $Ba(NO_3)_2$/cordierite without Pt at 350 °C in TM+ type measurement.

Table 1
Surface elemental composition measured with XPS before and after the $Ba(NO_3)_2$ decomposition experiment of 5 nmPt/$Ba(NO_3)_2$/cordierite

	Surface elemental composition (%)					N/Ba ratio
	Pt	Ba	N	C	O	
Before	36	3.1	4.0	36	21	1.29
After	15	9.1	4.5	32	40	0.49

analyzed to investigate the role of Pt, none of these products were detected. This indicated clearly that Pt was necessary to release NO_x from $Ba(NO_3)_2$ by H_2. This essential role of Pt for regeneration of NO_x was also elucidated recently by an analysis with in situ Fourier Transform Infrared spectroscopy [24]. It was found that both NO_x storage and regeneration needs Pt because the role of Pt of NO oxidation to NO_2 in NO_x storage process has been well known [25].

The surface elemental composition of the 5 nmPt/$Ba(NO_3)_2$/cordierite was measured using XPS before and after the above experiment as shown in Table 1. The reduction in the N/Ba ratio after the experiment confirmed the decomposition of $Ba(NO_3)_2$. When comparing the surface elemental composition before and after the measurement, it was found that the percentage of Pt decreased while the percentage of Ba increased. It is considered that the sintering of the Pt particles and encapsulation of the Pt particles cause the compositional change. The Pt in the $Ba(NO_3)_2$/cordierite was unstable and easily sintered into large particles. The phenomenon of the encapsulation of Pt particles by Ba has been observed after the reduction of a barium-based NSR catalyst [26].

3.2. Comparison of $Pt/Ba/Al_2O_3$ with Pt/Al_2O_3 in the TAP-type analyses

The results of TAP-type analyses of NSR using the pellet samples of $Pt/Ba/Al_2O_3$ and Pt/Al_2O_3 at 310 °C are shown in Fig. 4. When comparing the profile of NO and O_2 of $Pt/Ba/Al_2O_3$ to the one of Pt/Al_2O_3 (Fig. 4(a and c)), both the signal intensities of NO and O_2 of $Pt/Ba/Al_2O_3$ were less than the one of Pt/Al_2O_3. The product gases with H_2 injection as the result of NSR reaction were found in the case of $Pt/Ba/Al_2O_3$. These results indicated that the NO_x was stored in $Pt/Ba/Al_2O_3$ and the NSR reaction took place only in the case of $Pt/Ba/Al_2O_3$. In our experiment of Pt/Al_2O_3, the adsorption of NO_x on the Pt and Al_2O_3 [27,28] was not found.

Even though a large amount of NO and H_2O were observed in the TM+ type experiment using the 5 nmPt/$Ba(NO_3)_2$/cordierite sample (Fig. 3), NO was not observed here but a small amount of H_2O was. We suppose that almost all the NO was reduced to N_2 or NH_3 immediately and that the H_2O desorbed very slowly because of the strong affinity for alumina support. Therefore, the rate-limiting step during the rich phase is the decomposition of barium nitrate [29].

3.3. Influence of the amount of H_2

The influence of the amount of H_2 was investigated at 310 °C (Fig. 5). The amounts and ratios of the product and reactant gases changed in response to the increase in the amount of H_2 from 0 to 0.4 cm^3. NO and O_2 decreased and NH_3 increased with the amount of H_2 injection on the case between 0 and 0.3 cm^3 H_2 injection. In the case of 0.4 cm^3

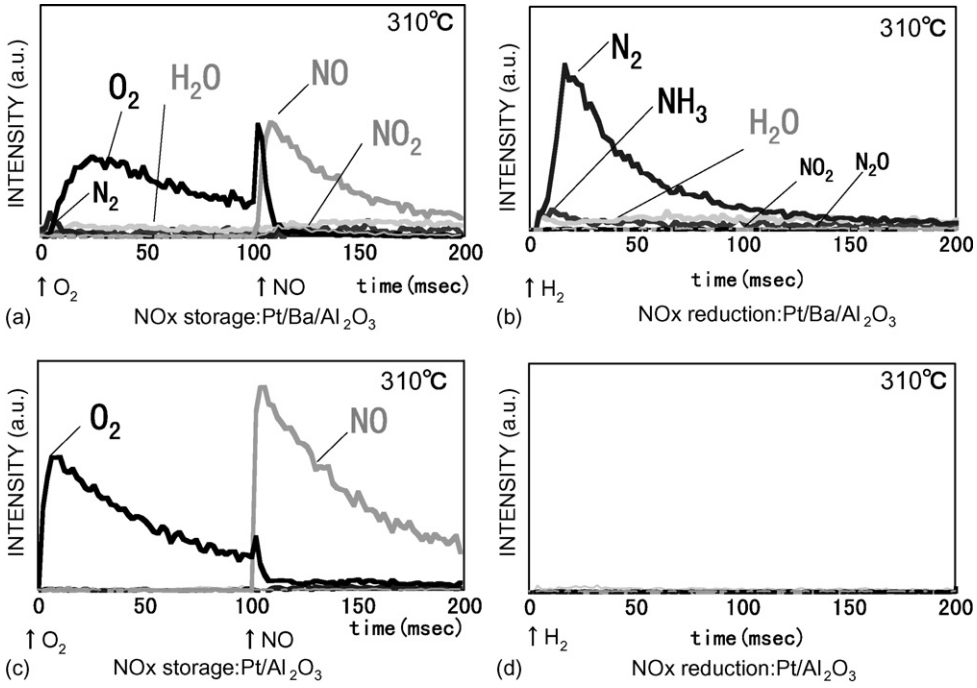

Fig. 4. TAP-type NSR analysis of $Pt/Ba/Al_2O_3$ and Pt/Al_2O_3 at 310 °C: (a) NO_x is stored in the $Pt/Ba/Al_2O_3$; (b) the stored NO_x is reduced by the 0.2 cm^3 pulses of H_2 gas, which is supplied 5 s after the NO_x storage procedure; (c and d) Pt/Al_2O_3 does not show the activity of NSR.

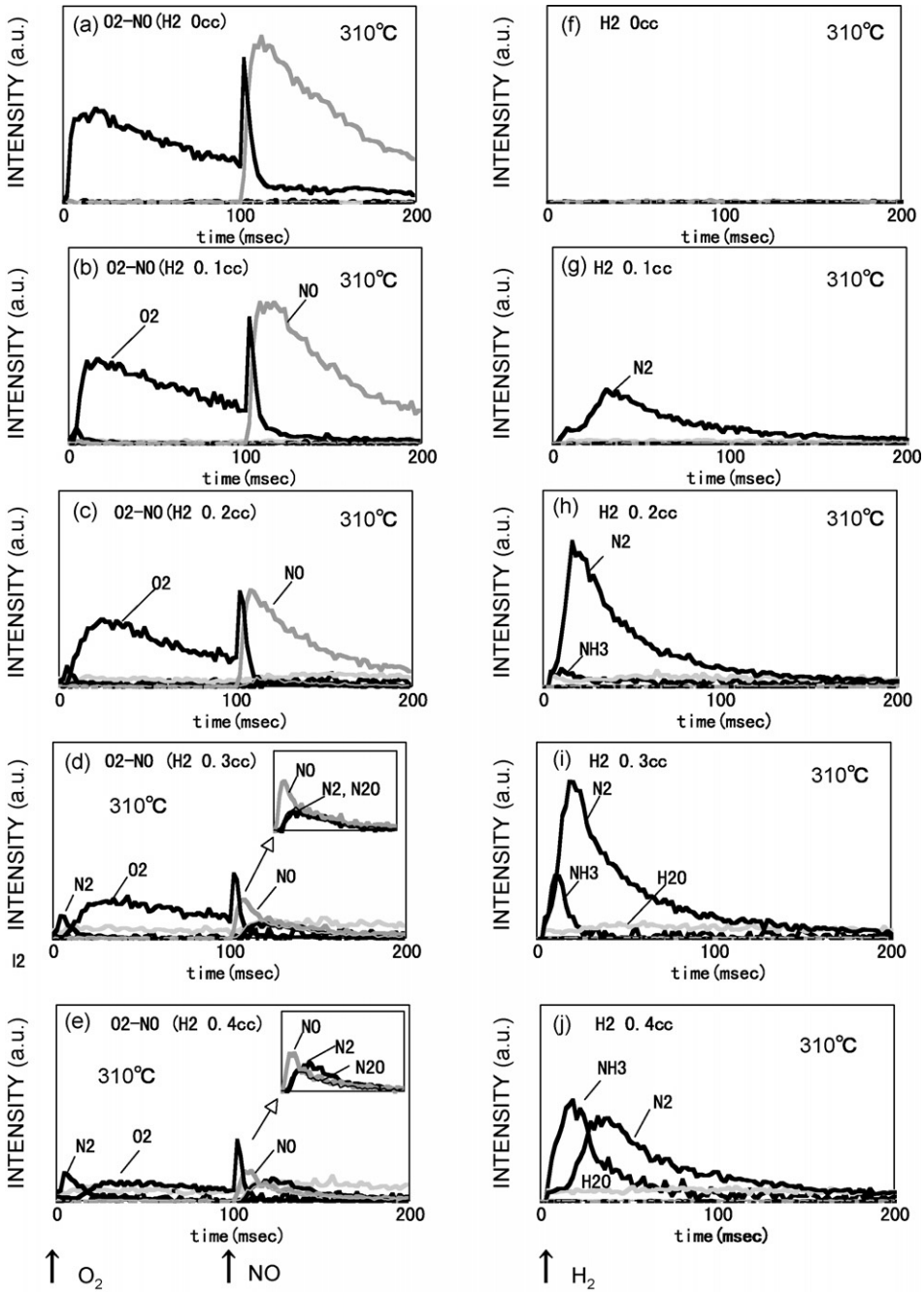

Fig. 5. Effect of the amount of H_2 on the NSR of $Pt/Ba/Al_2O_3$ at 310 °C. NO decreases and NH_3 increases with increasing amount of H_2.

H_2 injection (Fig. 5(j)), the amount of NH_3 increased and the amount of N_2 decreased in comparison with the result in Fig. 5(i).

We would like to just refer N_2 and N_2O after the injection of NO. In the case of 0.3 and 0.4 cm^3 H_2 injection, N_2 and N_2O were found after the injection of a NO pulse as shown in the magnified views in Fig. 5(d and e). When NO was injected, some of the injected NO was reduced to N_2 and N_2O at the Pt surface, which was still reduced or absorbed hydrogen despite the previous injection of O_2. This reaction was same as NO_x selective reduction and NO_x direct reduction.

3.4. Influence of temperature

We also investigated the influence of the amount of H_2 on both the products and reactants associated with NO_x storage and regeneration at temperatures of 440, 360, 310, 270 and 230 °C. In Fig. 6, the results are displayed in such a manner that the temperature varies in the vertical direction and the amount of H_2 varies in the horizontal direction. The N_2 intensity and the half of the NH_3 intensity were plotted against time. The leading edge of the time profile is generally steeper with increasing H_2 gas volume and increasing temperature. The ratio of NH_3 to N_2 also increases in the same way. We will discuss the rate of NO_x

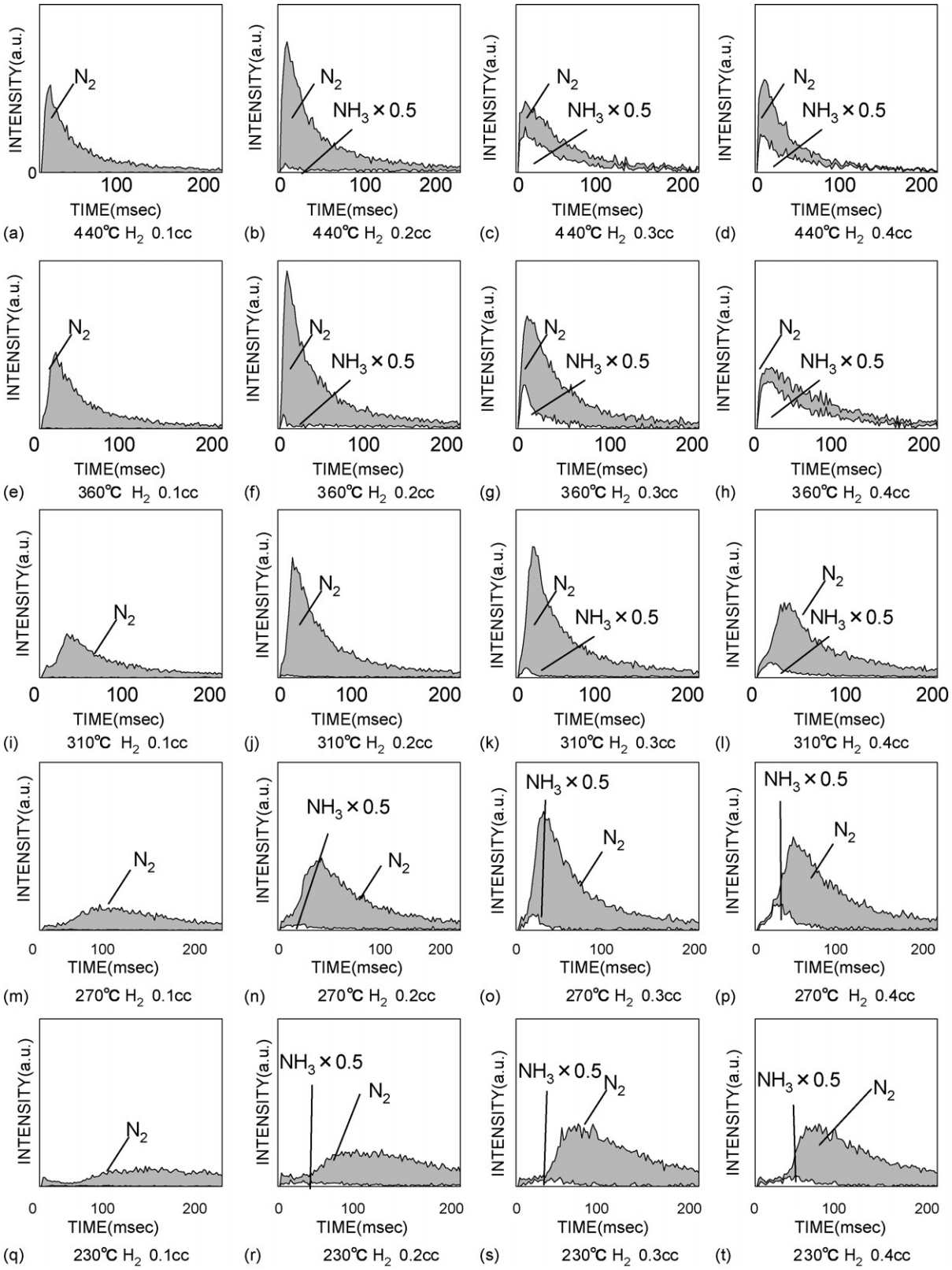

Fig. 6. Effect of temperature and amount of H_2 gas pulse on the time profiles of N_2 and NH_3 after supplying pulses of H_2 gas to $Pt/Ba/Al_2O_3$.

release and reduction, and the formation of NH_3 in the next section.

The amount of reduced NO_x was calculated at each temperature by subtracting NO profile of each amount of H_2 injection from the NO profile of 0 cm^3 of H_2 injection (Fig. 7). In the case of 0.3 and 0.4 cm^3 H_2 injection, the results agree with the previously known fact that the amount of NO_x storage is largest around 350 °C [11,30].

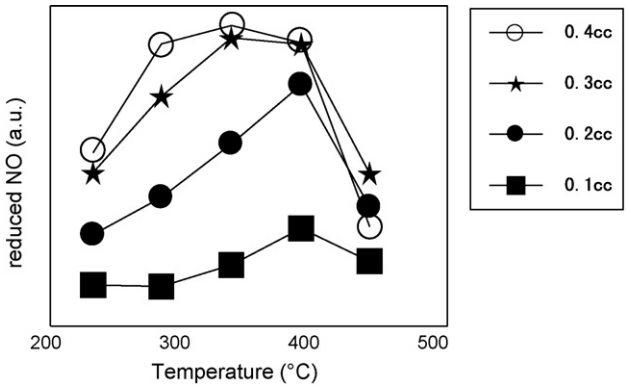

Fig. 7. Amount of reduced NO in the NSR analysis of $Pt/Ba/Al_2O_3$. The amount of reduced NO was calculated from the NO profile obtained from the analysis. The profiles are very similar to those of previously reported studies of NSR catalysts by conventional method.

4. Discussion

A NSR reaction with H_2 gas was investigated on a millisecond time scale using a flat 5 nm$Pt/Ba(NO_3)_2$/cordierite catalyst and a pellet of $Pt/Ba/Al_2O_3$. Instead of the direct comparison of the NO_x regeneration rate, we compared the profiles of $[N_2 + NH_3/2]$: the sum intensity of N_2 and half of NH_3. The profiles at each temperature were chosen so as to give almost the same amount of reduced NO_x, namely, 0.3, 0.2, 0.2, 0.2 and 0.3 cm^3 at 440, 360, 310, 270 and 230 °C, respectively (Fig. 8(a)). The $[N_2 + NH_3/2]$ increased as the temperature increases from 230 to 360 °C as described in the previous section and shown in Fig. 7. It was found that the NO_x regeneration rate became faster with increasing temperature, as shown by the leading edge of the normalized peak values becoming more rapid as the temperature increases (Fig. 8(b)).

To make the difference of the NO_x regeneration rate clearer, we tried to fit theoretical curves obtained from a simple reaction model to the $[N_2 + NH_3/2]$ profiles with a least square method. We assumed a two-step reaction model, whose formula was described as follows [31];

$$\frac{dC}{dt} = \frac{K_1 K_2}{(K_1 - K_2)} C_0(\exp(-K_2 t) - \exp(-K_1 t)).$$

Here, t stands for time and dC/dt stands for the intensity: $[N_2 + NH_3/2]$. The K_1 stands for the rate constant of the first step reaction and the K_2 stands for the one of the second step. C_0 is considered as the concentration of the stored NO_x. If we

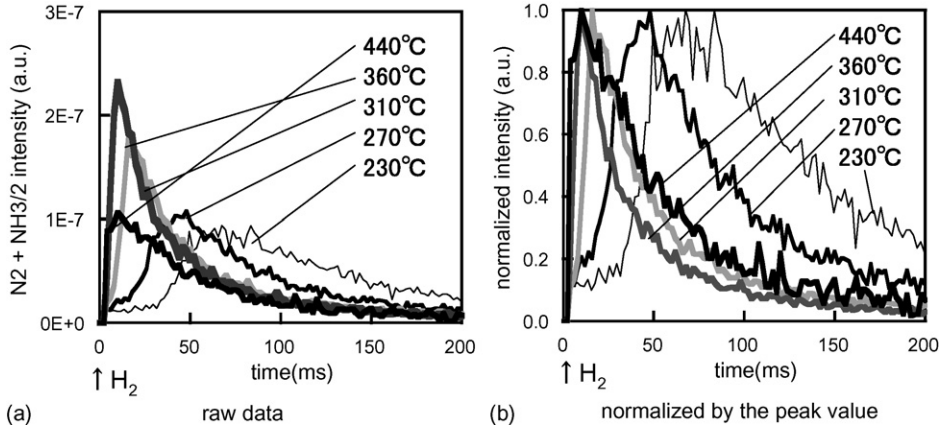

Fig. 8. Comparison of the $N_2 + NH_3/2$ profile (a) raw data and (b) normalized by the peak value.

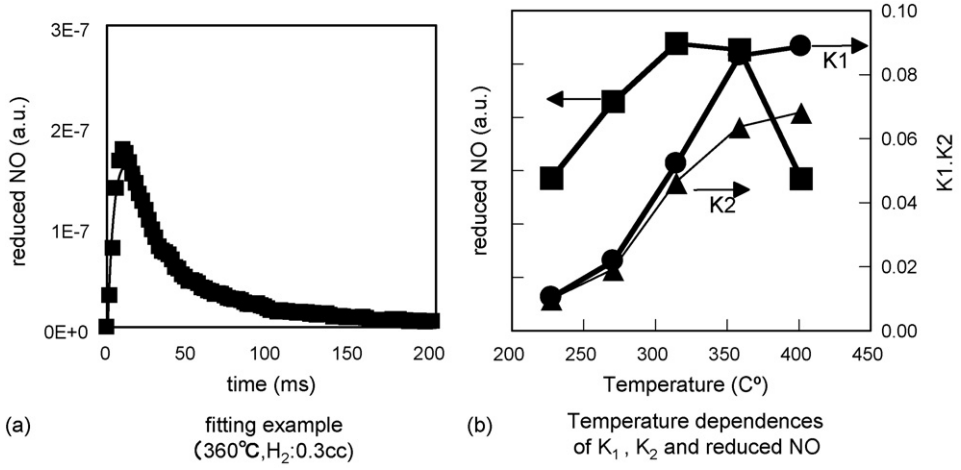

Fig. 9. Temperature dependences of the speed of NO_x regeneration and the amount of NO_x reduced using the data of 0.3 cm^3 of H_2 injection: (a) a fitting example of $N_2 + NH_3/2$ profile at 360 °C and (b) temperature dependences of K_1, K_2 and reduced NO: the same data in Fig. 7.

assume the first step as NO_x release and the second step as NO_x reduction, we are able to have the each rate constant.

An example of the fitting was shown in Fig. 9(a). The fitting seems to be successful. This fitting was performed to other time profiles of 0.3 cm^3 of H_2 injection. As shown in Fig. 9(b), the temperature dependences of K_1, K_2 and the amount of reduced NO for 0.3 cm^3 H_2 injection. The rate constant of K_1 and K_2 increased with increase in temperature from 230 to 440 °C, while the temperature dependence of the amount of reduced NO_x shows a maximum value around 300 °C. From this analysis, we suppose that the amount of reduced NO_x was decreased above 360 °C because of the decrease of the NO_x storage reactivity in $Pt/Ba/Al_2O_3$. If we assume the first step as NO_x release and the second step as NO_x reduction as mentioned above, it is considered that the rate constant of NO_x release and NO_x reduction between 230 and 310 °C are almost the same. When the temperature increase over 360 °C, the rate constant for NO_x release was found to be larger than the one for NO_x reduction. When the temperature was increased to 440 °C, a large amount of NH_3 was yielded. This NH_3 formation may be connected with the small rate of NO_x reduction over 360 °C.

At last, we would like to discuss NO storage reaction in NSR reaction and NH_3 formation in NO_x regeneration. It is clear that the profiles of O_2 and NO are different in the NO_x storage process shown in Fig. 5. The leading edge of the O_2 profile became gentler as the amount of H_2 increased, but the leading edge of the NO profile remained stable. This difference may indicate the difference between the reaction mechanisms of O_2 and NO with $Pt/Ba/Al_2O_3$, i.e., O_2 reacted with $Pt/Ba/Al_2O_3$ very fast and NO did not. When O_2 is injected to the $Pt/Ba/Al_2O_3$, the surface reduced by H_2 can adsorbed O_2 immediately. However, NO needs to react with dissociated oxygen for NO_x storage [32–34] and therefore the rate of NO reaction was not faster than the one of O_2 reaction.

A detailed report on NO_x regeneration in a NSR catalyst was recently published [35]. Although the report focused mainly on the effect of different reducing agents and precious metals, NH_3 formation in NO_x regeneration is also discussed. The result of the discussion showed that the amount of NH_3 increased as the temperature increased, which is the same as the result found in this work (Fig. 6). Another analysis showed that the generation of N_2 and the subsequent generation of NH_3 [36] accompany the introduction of H_2. The order in which these gases were generated is opposite to our result. The difference may be presumably due to the difference in the methods of H_2 introduction, i.e., pulsed injection in our case and step injection in the reference [36] in which the time profile of induced H_2 increases rapidly and then becomes stable. NH_3 formation tends to occur when the ratio of H_2 to NO increases [37]. In our study, the H_2/NO ratio is high just after H_2 pulse injection because the H_2 concentration is considered to be highest at that time and decreases rapidly from then on. On the other hand, in the study using a step profile for H_2, the H_2/NO ratio is low just after injection because a large amount of NO exists in the catalyst and the H_2/NO ratio is considered to increase gradually from then on. We regard this as the reason why the order of N_2 and NH_3 generation was different between the two works.

The formation of NH_3 and intermediate gases caused by CO and hydrocarbons [38] has often been discussed. This can be neglected in our case, because these reducing agents were not used in this study. However, the NH_3 may play an important role in NO_x release and reduction. Further analysis is necessary such as using NH_3 directly as a reducing agent for stored NO_x.

5. Conclusions

NO_x regeneration in an NSR catalyst with H_2 gas was investigated on a millisecond time scale. As for the gases produced as a result of NO_x regeneration, NO, N_2, NH_3 and H_2O, were detected from a flat 5 nm$Pt/Ba(NO_3)_2$/cordierite catalyst, though no products were detected from $Ba(NO_3)_2$/cordierite. It was found that Pt plays an important role in the NSR reaction and that NO was produced from decomposition of $Ba(NO_3)_2$ in the catalyst.

A NSR reaction using a pellet of $Pt/Ba/Al_2O_3$ as the catalyst was also investigated. The results were different from the analysis using the flat catalyst in which only a small amount of H_2O was detected because of the strong affinity for alumina support. NO was not observed since it was reduced into N_2. For a large amount of H_2 injection, a large amount of NH_3 was detected. Analysis both of the N_2 profile and their leading edges showed that the rate of NO_x regeneration increased with temperature and the amount H_2. We can analyze the NO_x regeneration process to separate two steps of the NO_x release and reduction by a detailed analysis of the time profiles using a two-step reaction model. From the result of the analysis, it is found that the rate constant for NO_x release increased as temperature increase.

References

[1] N. Miyoshi, S. Matsamoto, K. Katoh, T. Tanaka, J. Harada, N. Takahashi, K. Yakota, M. Sigiura, K. Kasahara, SAE Tech. Papers Ser. 950809, 1995.
[2] W. Bögner, M. Krämer, B. Kreutzsch, S. Pischinger, D. Voigtländer, G. Wenninger, F. Wirbeleit, M.S. Brogan, R.J. Brisley, D.E. Webster, Appl. Catal. B 7 (1995) 153.
[3] N. Takahashi, H. Shinjoh, T. Iijima, T. Suzuki, K. Yamazaki, K. Yokota, H. Suzuki, N. Miyoshi, S. Matsumoto, T. Tanizawa, T. Tanaka, S. Tateishi, K. Kasahara, Catal. Today 27 (1996) 63.
[4] E. Fridell, M. Skoglundh, S. Johansson, B. Westerberg, A. Törncrona, G. Smedler, Stud. Surf. Sci. Catal. 116 (1998) 537.
[5] H. Hirata, I. Hachisuka, Y. Ikeda, S. Tsuji, Si Matsumoto, Top. Catal. 16/17 (2001) 145.
[6] W.S. Epling, L.E. Campbell, A. Yezerets, N.W. Currier, J.E. Parks, Catal. Rev. Sci. Eng. 46 (2) (2004) 163.
[7] W.S. Epling, J.E. Parks, G.C. Campbell, A. Yezerets, N.W. Currier, L.E. Campbell, Catal. Today 96 (2004) 21.
[8] L. Olsson, B. Westerberg, H. Persson, E. Fridell, M. Skoglundh, B. Andersson, J. Phys. Chem. B 103 (1999) 10433.
[9] P. Denton, A. Giroir-Fendler, H. Praliaud, M. Primet, J. Catal. 189 (2) (2000) 410.
[10] S. Salasc, M. Skoglundh, E. Fridell, Appl. Catal. B 36 (2002) 145.
[11] H. Mahzoul, J.F. Brilhac, P. Gilot, Appl. Catal. B 20 (1999) 47.
[12] J. Sjöblom, K. Papadakis, D. Creaser, C.U.I. Odenbrand, Catal. Today 100 (2005) 243.
[13] L. Lietti, P. Forzatti, I. Nova, E. Tronconi, J. Catal. 204 (2001) 175.
[14] D. James, E. Fourré, M. Ishii, M. Bowker, Appl. Catal. B 45 (2003) 147.
[15] N.W. Cant, M.J. Patterson, Catal. Today 73 (2002) 271.

[16] T. Motohiro, Y. Kizaki, Y. Sakamoto, K. Higuchi, Y. Watanabe, S. Noda, Appl. Surf. Sci. 121/122 (1997) 319.
[17] T. Motohiro, Y. Kizaki, Y. Sakamoto, K. Higuchi, T. Tanabe, N. Takahashi, K. Yokota, H. Doi, M. Sugiura, S. Noda, Appl. Surf. Sci. 121/122 (1997) 323.
[18] Y. Sakamoto, Y. Kizaki, T. Motohiro, Y. Yokota, H. Sobukawa, M. Uenishi, H. Tanaka, M. Sugiura, J. Catal. 211 (2002) 157.
[19] T. Nakamura, Y. Sakamoto, K. Saji, J. Sakata, Sens. Actuators B 93 (2003) 214.
[20] M. Uenishi, H. Tanaka, M. Taniguchi, I. Tan, Y. Sakamoto, S. Matsunaga, K. Yokota, T. Kobayashi, Appl. Catal. A 296 (2005) 114.
[21] S.O. Shekhtman, G.S. Yablonsky, S. Chen, J.T. Gleaves, Chem. Eng. Sci. 54 (1999) 4371.
[22] S. Poulston, R.R. Rajaram, Catal. Today 81 (2003) 603.
[23] A. Cornu, R. Massot, Complication of Mass Spectral Data, second ed., Heyden & Son, 1975.
[24] Y. Su, M.D. Amiridis, Catal. Today 96 (2004) 31.
[25] R. Burch, T.C. Watling, Stud. Surf. Sci. 116 (1998) 199.
[26] P.T. Fanson, M.R. Horton, W.N. Delgass, J. Lauterbach, Appl. Catal. B 46 (2003) 393.
[27] T.J. Toops, D.B. Smith, W.P. Partridge, Appl. Catal. B 58 (2005) 245.
[28] D. Uy, K.A. Weigand, A.E. O'Neill, M.A. Dearth, W.H. Weber, J. Phys. Chem. B 106 (2002) 387.
[29] E. Fridell, M. Skoglundh, B. Westerberg, S. Johansson, G. Smedler, J. Catal. 183 (1999) 196.
[30] S. Matsumoto, Catal. Today 29 (1996) 43.
[31] K. Ohkubo, Y. Igari, S. Tomoda, I. Kusunoki, Surf. Sci. 260 (1992) 44.
[32] E. Fridell, H. Persson, B. Westerberg, L. Olsson, M. Skoglundh, Catal. Lett. 66 (2000) 71.
[33] L. Olsson, E. Fridell, M. Skoglundh, B. Andersson, Catal. Today 73 (2002) 263.
[34] X. Li, P. Vernoux, Appl. Catal. B 61 (2005) 267.
[35] H. Abdulhamid, E. Fridell, M. Skoglundh, Appl. Catal. B 62 (2005) 319.
[36] L. Castoldi, I. Nova, L. Lietti, P. Forzatti, Catal. Today 96 (2004) 43.
[37] Y.J. Mergler, B.E. Nieuwenhuys, Appl. Catal. B 12 (2–3) (1997) 95.
[38] T. Lesage, C. Verrier, P. Bazin, J. Saussey, M. Daturi, Phys. Chem. Chem. Phys. 5 (2003) 4435.